

# A model for the power required to access the H-mode in tokamaks and projections for ITER

R. Singh 1,2), P. Kaw 2), P.H. Diamond 1,3), H. Nordman 4), A. Loarte 5), D. Campbell 5), D. Bora 5)

1) WCI Center for Fusion Theory, National Fusion Research Institute, Republic of Korea; 2) Institute for Plasma Research, Bhat Gandhinagar-2382 428, India; 3) CMTFO and CASS, University of California San Diego, USA; 4) Department of Earth and Space Sciences, Chalmers University of Technology, SE-412 96 Göteborg, Sweden; 5) ITER Organization, Route de Vinon Sur Verdon, A. 13115 Saint Paul Lez Durance, France

E-mail contact person: [rsingh129@yahoo.co.in](mailto:rsingh129@yahoo.co.in)

**Abstract.** We present a new model for the low (L) to high (H) mode transition which can analytically predict the transition power threshold ( $P_{LH}$ ) as a function of plasma parameters. High poloidal mode number drift resistive ballooning mode (high-m DRBM) is assumed to be a dominant turbulent process in the L-mode edge region [i.e. in the vicinity of last closed flux surface (LCFS)]. We derive an edge power balance relation by evaluating power flux from the core and obtain  $P_{LH}$  by imposing the condition of turbulence suppression by  $\mathbf{E} \times \mathbf{B}$  shear. Evaluation of  $P_{LH}$  shows reasonable agreements with experimental data for many existing tokamaks. Increase of  $P_{LH}$  at low density (i.e. the existence of roll-over density in  $P_{LH}$  vs. density curves) is shown to originate from the longer scale length of density profile than that of temperature, and the reduction of the ratio of ion to electron temperature in dominant electron heating. Finally, a prediction of  $P_{LH}$  for ITER is presented.

## 1. Introduction

Elucidating the physics of the L- to H-mode transition is almost 30 years-old endeavour since its first discovery on ASDEX [1]. The most important driver for these efforts is that the H-mode, which is characterized by the presence of edge transport barriers (ETB), yields high fusion performance, given the stiffness of the core temperature profile. This is particularly important to ITER which aims at realization of high fusion gain deuterium-tritium (DT) plasmas. H-mode operation in ITER is also planned even in the non-active (H and He) and the DD phases to characterize H-mode plasmas in ITER-scale and to develop reliable edge localized modes (ELM) control schemes well before the DT operation phase. Key physical concepts involved in the L-H transition physics have been rapidly developed for the past two decades. The most important concept for L-H transition physics is the suppression/reduction of turbulence by shear  $\mathbf{E} \times \mathbf{B}$  flow [2-3]. Unfortunately, however, we still suffer from the lack of theory-based analytic models giving a reliable prediction of the L-H transition power threshold ( $P_{th}$ ). In particular, this is an issue in ITER planning to achieve H-mode in the non-active phase with limited power available.

Given the absence of a reliable predictive model allowing a quantitative evaluation of  $P_{th}$  in ITER, experimentalists have relied on some empirical scalings which were derived based on a statistical analysis of experimental data in present tokamaks. In this approach,  $P_{th}$  has been characterised for hydrogenic plasmas and found to depend on atomic mass ( $A_i$ ), plasma density ( $n$ ), toroidal field ( $B_T$ ) and plasma surface ( $S$ ) [4]:

$$P_{th} = 0.0976 A_i^{-1} \left[ n(10^{20} m^{-3}) \right]^{0.717} \left[ B_T(T) \right]^{0.803} \left[ S(m^2) \right]^{0.941} \quad (1)$$

A drawback of these empirical relations, though useful, available in the literature [such as Eq. (1)] is that it cannot reproduce the increasing tendency of  $P_{th}$  at low density (i.e.  $P_{th} \propto n^{-\alpha}$  with  $\alpha > 0$ ).

For helium plasmas the power threshold is known to be intermediate between those of hydrogen and deuterium plasmas (a factor of 2 higher than for deuterium) but the precise value varies across tokamak experimental conditions and with the plasma density for a given device. Consequently, the prediction of  $P_{th}$  in ITER remains largely uncertain. To improve this present situation, we present a simple model for power threshold to achieve H-mode which is testable in present experiments and gives rise to a quantitative prediction of  $P_{th}$ . In Section 2, we develop an analytic model of the L-H transition. We assume that high-m DRBM [5-7] is a dominant turbulent process in the L-mode edge. We derive an edge power balance relation by evaluating power flux from the core and obtain  $P_{LH}$  by imposing the condition of turbulence suppression by  $\mathbf{E} \times \mathbf{B}$  shear. In Sec. 3, we evaluate  $P_{th}$  for various present tokamaks and predict it for ITER. We identify the origin of increasing tendency of  $P_{th}$  at low density. We conclude our paper in Sec. 4 with a brief summary of the main results.

## 2. A power balance model for L-H transition

We start with the following conjectures. First, we assume that heat flux from a core plasma is transported through a narrow region near the last closed flux surface (LCFS) by convection, conduction and radiation processes. This narrow region is assumed to be order of temperature scale length, which is 4-5 % of minor radius ( $a$ ), (i.e.  $\Delta_R / L_T \ll 1$ ), where  $\Delta_R = a - r$  is the width of the narrow region and  $L_T = -T_e / \nabla_r T_e$ . In L-mode discharges, the density scale length is smaller than the temperature scale length (i.e.  $L_T > L_n (= -n / \nabla_r n)$ ).  $L_n$  in the vicinity of LCFS is determined by ionization and charge exchanges processes. This can be written from 1-D equations for neutral and plasma particles by taking the edge recycling factor as unity at the boundary ( $r = a$ ) [8-9], resulting in  $L_n \approx 1 / n\sigma_*$ . Here  $\sigma_* = \sqrt{m_i(\kappa_i + \kappa_{cx})\kappa_i / T}$ ,  $\kappa_i = \langle \sigma v \rangle_{ion}$  and  $\kappa_{cx} = \langle \sigma v \rangle_{cx}$  are the rate coefficients of ionization and charge exchange processes and  $\sigma_* \approx 3.6 \times 10^{-19} m^2$ . Second, we further assume that the power loss due to convection and conduction processes is dominated by nonlinear properties of high poloidal mode number drift resistive ballooning mode (high-m DRBM) [5-7]. Note that other modes like the electromagnetic drift wave also called as drift Alfvén modes are stable in a sheared slab and could be excited by nonlinear effects [10] and moreover the simple Alfvén wave is always stable in the vicinity of LCFS. The high-m DRBM has similar growth rate to ideal ballooning modes even when  $\beta$  less than  $\beta_c$  for the ideal MHD ballooning. Here  $\beta = 2\mu_0 P / B^2$ ,  $P$ , the total kinetic pressure,  $\beta_c \approx q^2 R [1 + \tau_i + \eta] / L_n$ ,  $q = rB_T / RB_p$ , the safety factor,  $R$ , the major radius of tokamak,  $\eta = L_n / L_T$ ,  $\tau_i = T_i / T_e$ ,  $B \approx B_T$  and  $B_p$ , the toroidal and poloidal magnetic fields. The radial correlation length is determined by balancing the compression of polarization current and parallel electron current. The growth rate ( $\gamma$ ) and radial correlation length ( $L_0$ ) of DRBM are given by [10, 12],

$$\gamma = \sqrt{\frac{2c_{sH}^2(1 + \tau_i)}{RL_n A_i}}; \quad L_0 \approx \left( \frac{q^2 v_e \rho_{sH} R}{2\Omega_e \hat{s}^2} \right)^{1/2} \left( \frac{2R(1 + \tau_i) A_i}{L_n} \right)^{1/4} \quad (2)$$

Here  $c_{sH} = \sqrt{T_e / m_H} = 3.09 \times 10^5 [T_e (KeV)]^{1/2} m$ , the thermal velocity of hydrogen ion,  $A_i$  the atomic mass,  $\nu_e$ , the electron-ion collision frequency, for singly charged ions,  $\nu_e^{-1} = \tau_e = 6.4 \times 10^{14} [T (KeV)]^{3/2} / n (m) s$ ,  $n$ , the plasma density in the edge,  $\Omega_e$ , the electron gyrofrequency,  $\hat{s}$ , the magnetic shear. Using the mixing length argument the particle and thermal diffusion coefficients can readily be written as

$$D \approx \chi_e = \gamma L_0^2 \approx (1 + \tau_i) (q^2 R / \hat{s}^2 L_n) \nu_e \rho_e^2, \quad (3)$$

Here  $\rho_e$  is the electron gyro-radius, we use Fick's law and write the particle and thermal fluxes as  $\Gamma_n = -D \partial n / \partial r$   $\Gamma_e = -\chi_e \partial T_e / \partial r$ . Under the assumptions of dominant of high-m DRBM transport the edge power balance can be re-written as:

$$\begin{aligned} P_{th}^{core} &= (T \Gamma_n + n \Gamma_e) \times S + P_R \\ &= (1 + \tau_i) [q / \hat{s}]^2 R \nu_e \rho_e^2 n^3 T_e \sigma_*^2 S [1 + 1 / (n \sigma_* L_T)] + P_R \end{aligned} \quad (4)$$

Here  $S = 2\pi R \times 2\pi a \sqrt{(1 + \kappa^2) / 2}$ , the surface area of plasma column,  $\kappa$ , the plasma elongation and  $P_R$ , the radiative power in the vicinity of LCMS and  $P_R$  can be written as

$$P_R = n_I n R_T \times V = Z_n n^2 R_T V; \quad V = 4\pi^2 a R \Delta_R; \quad Z_I = \sum_I n_I / n \approx (0.02 - 0.3) \quad (4)$$

We normalize the volumetric radiation ( $R_T$ ) from the edge region of width  $\Delta_R$  by  $10^{-30} MW m^3$ , the edge plasma density ( $n$ ) by  $10^{20} m^{-3}$  and  $n_I / n = 0.01$ , the impurity density is 1% of plasma density. Then the radiative power ( $P_R$ ) in  $MW$  can be expressed as

$$P_R (MW) = 3.95 Z_n (10^{-2}) [n (10^{20} m^{-3})]^2 R_T (10^{-39} MW m^3) a(m) R(m) \Delta_R(m) \quad (6)$$

The power balance Eq. (4) can be re-written as:

$$P_{th}^{core} (MW) = 0.286 \times 10^{-44} (1 + \tau_i) \left( \frac{nqR}{B} \right)^2 \frac{n^2 \sigma_*^2 S}{R} [T_e (KeV)]^{1/2} \left( 1 + \frac{1}{n \sigma_* L_T} \right) + P_R (MW) \quad (7)$$

In Eq. (7), the factor  $nqR / B$  can be further expressed as a Hugill or Greenwald density limit,

$$\left( \frac{nqR}{B} \right)^2 = (2\pi)^{-2} \times 10^{42} \left[ \frac{\bar{n} (10^{20} m^{-3})}{I (MA) / \pi a^2} \right]^2 \left( \frac{n}{\bar{n}} \right)^2 \left( \frac{1 + \kappa^2}{2} \right) \quad (8)$$

Here  $n$  and  $\bar{n}$  are the edge density in the narrow region and line averaged density, the poloidal magnetic field ( $B_p$ ) in the definition of safety factor is evaluated by

$$\text{relation } 2\pi a B_p \sqrt{(1 + \kappa^2) / 2} = \mu_o I, \quad \mu_o = 4\pi \times 10^{-7} (Tm / A).$$

Combining equation (7) and (8), the Eq. (7) can be re-stated as

$$\begin{aligned} P_{th}^{core} (MW) &= 0.286 \times 10^{-2} (1 + \tau_i) \left[ \frac{\bar{n} (10^{20} m^{-3})}{\hat{s} (I (MA) / \pi a^2)} \right]^2 \left[ \frac{n}{\bar{n}} \right]^2 \left[ \frac{1 + \kappa^2}{2} \right]^{3/2} \\ &\quad \times a \times [T_e (KeV)]^{1/2} \times (n \sigma_*)^2 \times \left( 1 + \frac{1}{n \sigma_* L_T} \right) + P_R (MW) \end{aligned} \quad (9)$$

To evaluate the temperature in the edge region, we assume that the suppression of high-m DRBM transport occurs when the ExB rotational shear exceeds the typical autocorrelation time of the turbulence (i.e.  $V_E' > (\Delta_r k_\theta \tau_c)^{-1}$ ) [3], where  $\Delta_r$  is the radial correlation length,  $k_\theta$

is the poloidal wave vector,  $\Delta_r k_\theta \sim 1$ ,  $(\tau_c)^{-1} \approx \gamma^{in} \approx \sqrt{2c_{sH}^2(1+\tau_i)/RL_n A_i}$  of DRBM. The  $V_E$  shear rotation is obtained from radial force balance equation. For  $L_T > L_n$  and weak toroidal rotation, the expression for  $V_E'$  can be expressed as

$$V_E' \approx \frac{T_i(\nabla_r n)^2}{eZBn^2} = \frac{\tau_i T_e}{eZBL_n^2} > \sqrt{\frac{2c_{sH}^2(1+\tau_i)}{RL_n A_i}} \quad (10)$$

Eliminating  $L_n \approx 1/n\sigma_*$  from (10), we get the expression for temperature, which implies a temperature threshold to be exceeded as

$$[T_e(KeV)]^{1/2} \geq 3.09 \times 10^2 B(T) \left[ \frac{Z}{\tau_i} \right] \left[ \frac{1}{n(m^{-3})\sigma_*} \right]^{3/2} \sqrt{\frac{2(1+\tau_i)}{A_i R}} \quad (11)$$

The combination of this requirement with the power balance expression in Eq. (9) provides an expression for the H-mode threshold power,

$$P_{th}(MW) > 7.5 \times \left[ \frac{\bar{n}(10^{20} m^{-3})}{\hat{s} \times I(MA) / \pi a^2} \right]^2 \left[ \frac{n}{\bar{n}} \right]^2 \times \varepsilon \times [R(m)]^{1/2} \times B(T) \times [n(10^{20} m^{-3})]^{1/2} \times \left[ \frac{Z}{\tau_i A_i^{1/2}} \right] \\ (1+\tau_i)^{3/2} \times \left[ \frac{(1+\kappa^2)}{2} \right]^{3/2} \times [\sigma_* (3.6 \times 10^{-19} m^2)]^{1/2} \times \left[ 1 + \frac{1}{36 \times n(10^{20} m^{-3}) \sigma_* (3.6 \times 10^{-19} m^2) \times L_T} \right] \\ + 3.95 \times Z_n (10^{-2}) \times [n(10^{20} m^{-3})]^2 \times R_T (10^{-39} MW m^3) \times a(m) \times R(m) \times \Delta_R(m) \quad (12)$$

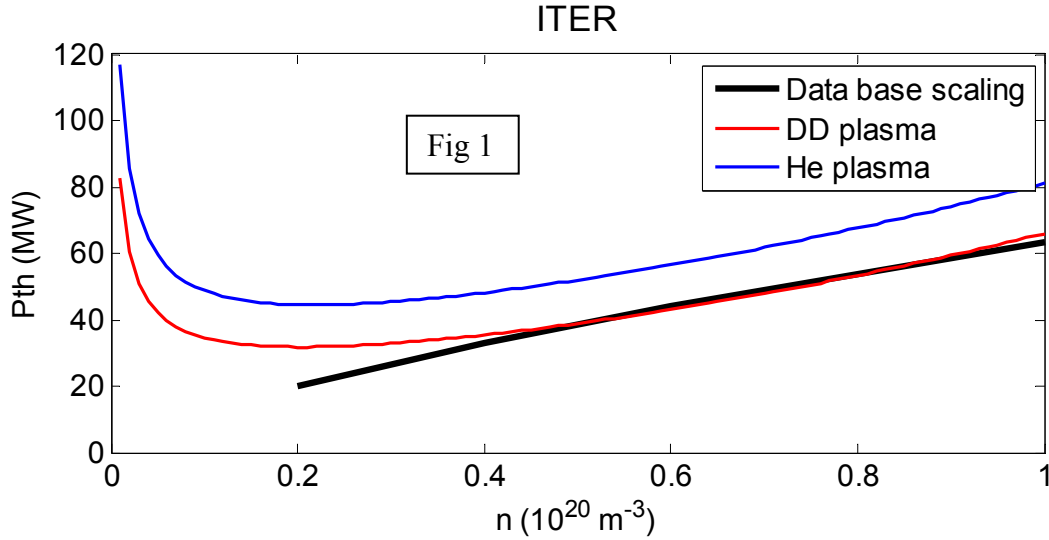
Eq. (12) can also be used to identify the physics processes leading to the increase of the H-mode threshold at low density: a) the scale length of density profile becomes longer than that of the temperature, b) power loss due to diffusive process dominates over convective loss, and c) the ratio of ion to electron temperature decreases for electron heated plasmas because of the inefficiency of equipartition at these densities as found in experiments [11-12]. The first two effects are relevant to ITER while the last one is not; even for L-mode conditions the equipartition term is dominant in ITER and  $T_e = T_i$  is expected [13]. In addition, Eq. (12) also predicts the H-mode power threshold scaling on atomic charge, atomic mass and geometric mean of ionization and charge-exchange processes,

$$P \propto \left[ \frac{Z^2 \sigma_*}{A_i} \right]^{1/2} \quad (13)$$

This predicts the He H-mode power threshold for similar plasma conditions to be between the one for H and D plasmas with the exact magnitude depending on the plasma temperature before the H-mode transition (which affects the ratio of  $\sigma_0(He)$  to  $\sigma_0(H)$  in qualitative agreement with experimental results. Eq. (12) can be used to evaluate the H-mode power threshold requirements for the existing devices and predictions for ITER.

### 3. Calculation of L-H transition power threshold

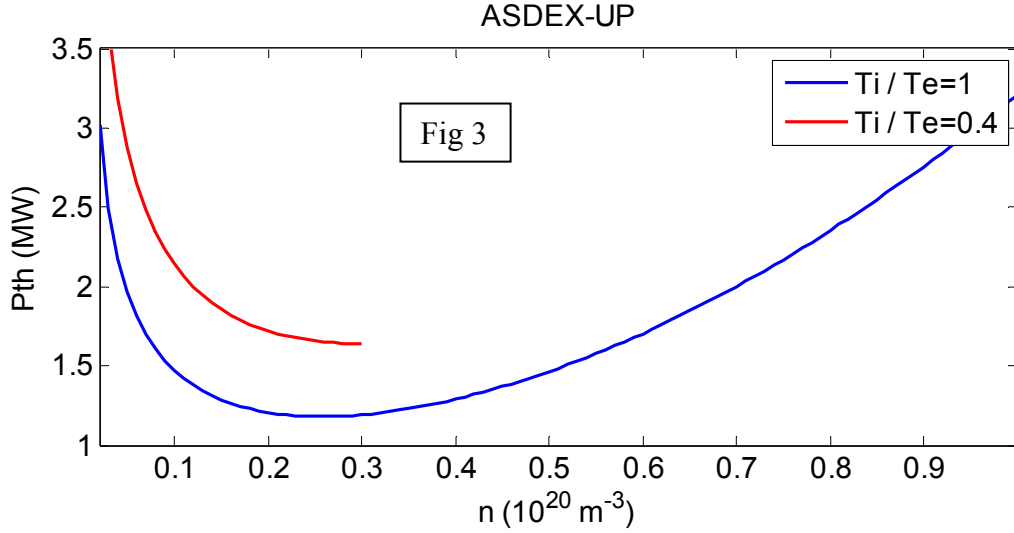
**ITER:** Predictions for H-mode power threshold as function of edge density for Helium and Deuterium plasmas are shown in Fig. 1 for typical ITER plasma parameters:  $R=6.2m$ ,  $a=2m$ ,  $\kappa=1.7$ ,  $B=5.3T$ ,  $I_p=15MA$ ,  $T_i/T_e=1.0$ ,  $\bar{n}=0.92 \times 10^{20} m^{-3}$ ,  $n/\bar{n}=0.66$ ,  $L_T/a=0.05$ ,  $Z_l=0.02$ ,  $R_T=3 \times 10^{-30} MW m^3$



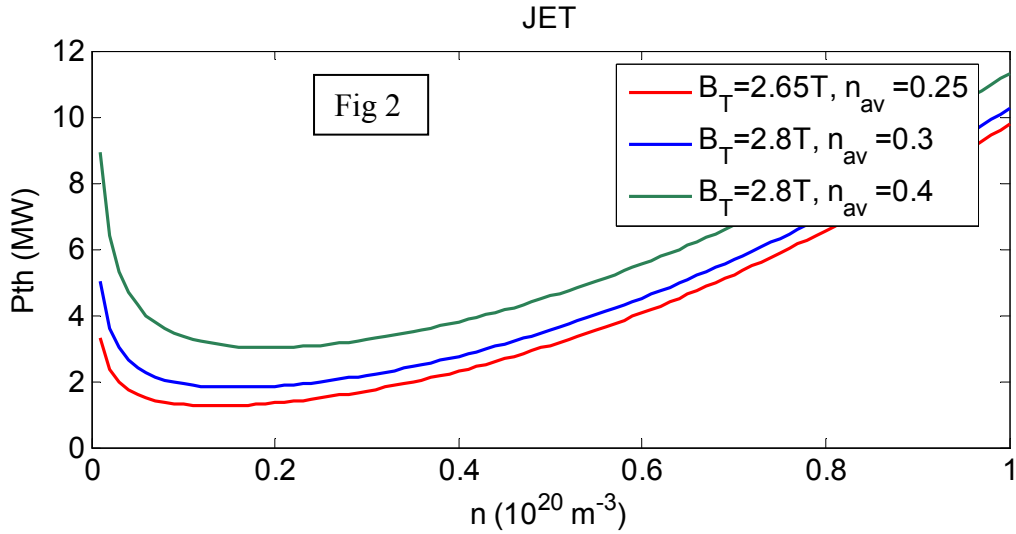
This clearly indicates the atomic mass ( $A_i$ ) dependent H-mode power threshold. In Fig. (1), the black line is drawn from empirical formula given by Eq. (1) [4]. We also observe the parameters  $\bar{n}/n_G$  ( $n_G = I(MA)/\pi a^2$  is the Greenwald's density) and  $n_{edge}/\bar{n}$  play significant role in determining H-mode power threshold. The power threshold is smaller at the lower values of both ratios.

Finally, in order to test our model, we further give the plots for H-mode power threshold ( $P_{th}$ ) versus plasma density ( $n$ ) from Eq. (14) for various machines like, ASDEX-UP, JET, D-IIIID, ALCATOR C MOD, and EAST superconducting tokamak.

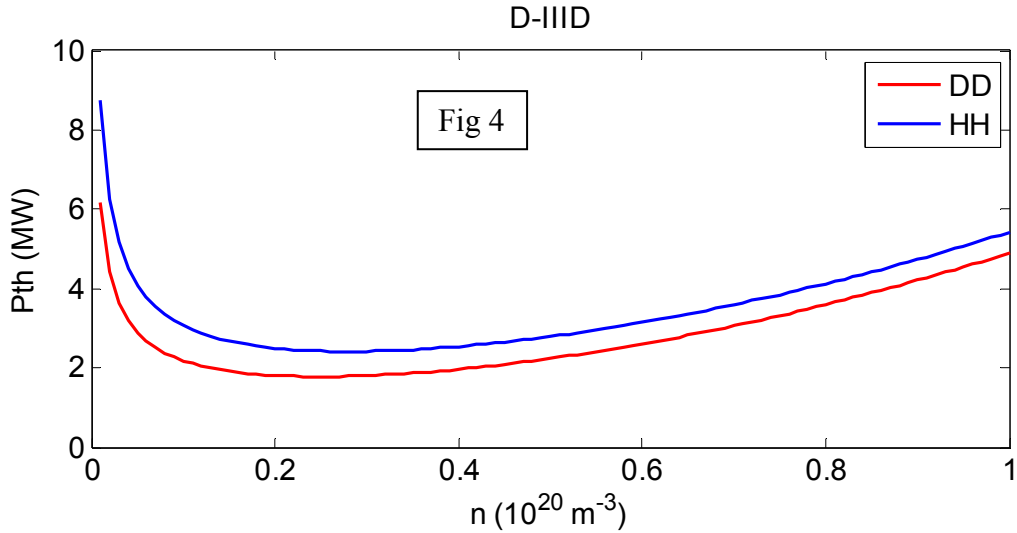
**ASDEX-UP:** The H-mode power threshold of AUG [16] for plasma parameters:  $R = 1.63m$ ,  $a = 0.5m$ ,  $\kappa = 1.7$ ,  $B = 2.3T$ ,  $I_p = 3MA$ ,  $A_i = 2.0$ ,  $T_i/T_e = 1.0$ ,  $\bar{n} = 0.35 \times 10^{20} m^{-3}$ ,  $n/\bar{n} = 1/2$ ,  $L_T/a = 0.05$ ,  $Z_I = 0.05$ ,  $R_T = 3 \times 10^{-30} MW m^3$ , is shown in Fig. 3. At low density, dependence of temperature ratio (i.e.  $T_i/T_e = 0.4$ ) is given by red line. This clearly shows that the higher power is required to achieve H-mode when ion temperature is lower than electron temperature. Recently this has been observed in electron heated plasmas experiments [11] at low density [i.e.  $n(10^{20} m^{-3}) < 0.3$ ]. For temperature ratio  $T_i/T_e = 1.0$ , the H-mode power threshold represent by blue line.



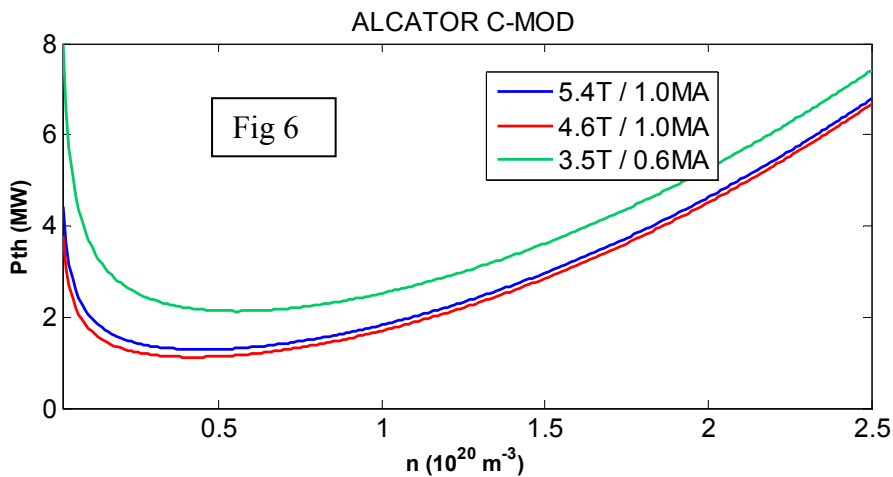
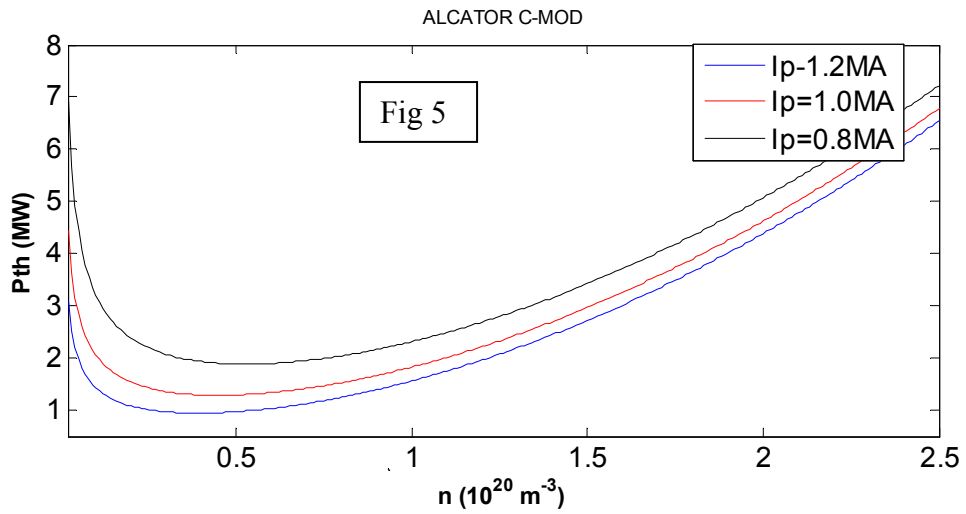
**JET:** Predictions for H-mode power threshold as function of edge density ( $n$ ) for  $B = (2.5, 2.8)T$  and line averaged density  $\bar{n} = (0.25, 0.30, 0.4) \times 10^{20} m^{-3}$  in JET [4] are shown in Fig. 2 for typical DD plasma parameters:  $R = 3m$ ,  $a = 1.0m$ ,  $\kappa = 1.7$ ,  $I_p = 3MA$ ,  $T_i/T_e = 1.0$ ,  $\bar{n} = 0.35 \times 10^{20} m^{-3}$ ,  $n/\bar{n} = 1/2$ ,  $L_T/a = 0.05$ ,  $Z_I = 0.05$ ,  $R_T = 3 \times 10^{-30} MW m^3$  [2].



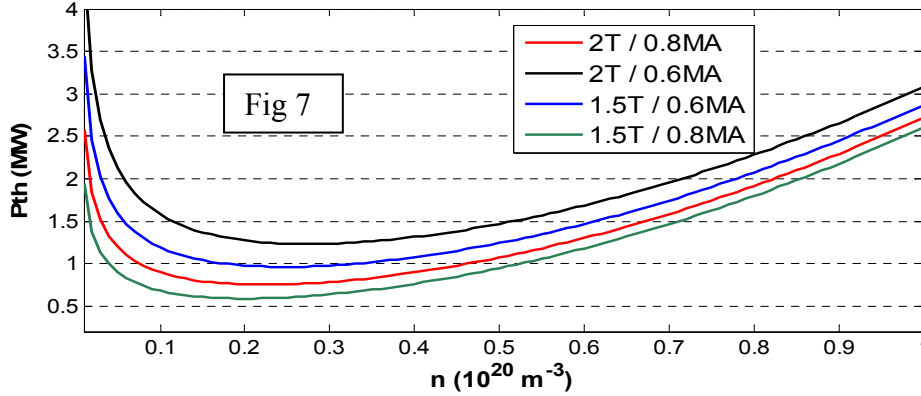
**D-IIID:** Atomic mass dependence power threshold ( $P_{th}$ ) versus edge density ( $n$ ) for D-IIID [17] plasma parameters  $R = 1.7m$ ,  $a = 0.6m$ ,  $\kappa = 1.7$ ,  $B = 1.65T$ ,  $I_p = 1.0MA$ ,  $A_i = 2$ ,  $T_i/T_e = 1.0$ ,  $\bar{n} = 0.35 \times 10^{20} m^{-3}$ ,  $n/\bar{n} = 1/2$ ,  $L_T/a = 0.05$ ,  $Z_I = 0.1$ ,  $R_T = 3 \times 10^{-30} MW m^3$ , is shown in Fig. 4



**ALCATOR C-MOD:** Fig. 5 shows  $P_{th}$  versus  $n$  from varying current  $I_p$  (0.8, 1.0, 1.2) MA for ALCATOR C-MOD [14] plasma parameters  $R=0.67\text{m}$ ,  $a=0.22\text{m}$ ,  $\kappa=1.55$ ,  $B=5.4\text{T}$ ,  $A_i=2$ ,  $T_i/T_e=1.0$ ,  $\bar{n}=1.2 \times 10^{20} \text{ m}^{-3}$ ,  $n/\bar{n}=1/2$ ,  $L_T/a=0.05$ ,  $Z_I=0.1$ ,  $R_T=1.5 \times 10^{-38} \text{ MW m}^3$ . Fig. 6 represents the power threshold ( $P_{th}$ ) from  $B$  (3.5T, 4.6T, 5.4T) and  $I_p$  (0.6MA, 1.0MA) versus ( $n$ ). Both figures (5) and (6) show the lower power threshold at higher plasma current and lower magnetic field.



**EAST:** Estimates for  $P_{th}$  as a function of edge density form lower  $B(1.5T, 2T)$  and  $I_p(0.6MA, 0.8MA)$  for H-mode discharges in EAST superconducting tokamak [15] are shown in Fig. 7. Typical plasma parameters for EAST tokamak taken are:  $R=1.88m$ ,  $a=0.45m$ ,  $\kappa=1.7$ ,  $B=(1.5-2)T$ ,  $I_p=(0.6-0.8)MA$ ,  $A_i=2$ ,  $T_i/T_e=1.0$ ,  $\bar{n}=0.3 \times 10^{20} m^{-3}$ ,  $n/\bar{n}=1/2$ ,  $L_T/a=0.05$ ,  $Z_I=0.1$ ,  $R_T=3 \times 10^{-39} MW m^3$ . Green line clearly indicates the lowest threshold at higher current and lower toroidal magnetic field.



Note that the ratio of edge density ( $n$ ) to line averaged density ( $\bar{n}$ ) has as similar magnitude for all devices and is estimated by assuming  $n/\bar{n}=1/2$ . It is a common observation in most of tokamaks that  $n/\bar{n} < 1$ . We also observe that the parameters  $n/\bar{n}$  and  $\bar{n}/(I/\pi a^2)$  played a critical role in accessing the H- mode at lower power. H-mode could be achieved at lower power by keeping the lower value of the parameters  $n/\bar{n}$  and/or  $\bar{n}/(I/\pi a^2)$ . This could be tested experimentally by increasing plasma current ( $I_p$ ) at constant line averaged density ( $\bar{n}$ ) or at fixed plasma current, the density ( $\bar{n}$ ) could be increased by different fuelling techniques such as gas puffing, molecular beam injection, and pallet injection.

#### 4. Conclusions

In conclusion, we have developed a new model, which determines the power to access the H-mode in tokamaks. It is based on postulates that a) the power out flux from core plasma is transported through the narrow region in the edge near the LCMS by convection, conduction and radiation processes. b) In this narrow region, the density scale length is shorter than temperature length scale and determines by ionization and charge-exchange process. The power loss due to convection and conduction processes is determined by nonlinear properties of DRBM. c) Critical edge temperature is evaluated by suppression of DRBM due to  $E \times B$  shear rotation condition. The H-mode power threshold for the existing tokamaks like ASDEX-UP, JET, D-IIID, ALCATOR C-MOD, EAST superconducting tokamak are calculated and found to be in reasonable agreement with the measurements. The predictions for ITER are shown that the power required, from low line averaged density  $\bar{n}(0.5-1.0) \times 10^{20} m^{-3}$ , to achieve H-mode is typically  $P_{th}(40-55)MW$  for DD plasma. In HH plasma, H-mode power could be 1.5 times larger than DD plasma. The model also points to the vital role of the ratio of density in the vicinity of LCMS to the line averaged



density (i.e.  $n_{edge} / \bar{n}$ ) and the ratio of  $\bar{n}$  to the Greenwald density. The power threshold is smaller at the lower values of both ratios. This also suggests the importance of deep particle fuelling over gas puffing in the edge and plasma current.

### Acknowledgements

This research was supported by the Ministry of Education, Science and Technology of Korea via WCI project 2009-0001, by the U. S. DOE Contract No. DE-FC02-08ER54959, and the J.-I. G. Foundation for Cutting Edge Research.

### References

1. Wagner F. *et al* Phys. Rev. Lett **49** (1982) 1408
2. Diamond P. H. *et al* Plasma Phys. Controlled Fusion **47** (2005) R35
3. Biglari H., Diamond P. H. *et al* Phys. Fluids **B2** (1990) 1
4. Martin Y. R. *et al* Journal of Physics: Conference Series **123** (2008) 012033
5. Novakovskii S. V. *et al* Phys. Plasmas **2** (1995) 781
6. Roger B. N. *et al* Phys. Rev. Lett **81** (1998) 4396
7. Singh R. *et al* Phys. Plasmas **12** (2005) 092307
8. Choudhury S. R and Kaw P. K., Phys. Plasmas **B1** (1989) 1646
9. Tokar M. Z., Phys. Rev. Lett **9** (2003) 095001
10. Scott B. D. **B4** (1992) 2468
11. Sauter P. *et al* Nucl Fusion **51** (2011) 072001
12. Ryter F. *et al* Proc. 13<sup>th</sup> H-mode workshop, Oxford, UK, 2011
13. Polevoi A. *et al* Proc. 23<sup>rd</sup> IAEA Fusion Energy Conf., Daejeon, Rep. of Korea, 2010
14. Ma Y. *et al* Nucl Fusion **52** (2012) 023010
15. Xu G. S. *et al* Nucl Fusion **51** (2011) 072001;